Progress In Electromagnetics Research C, Vol. 70, 135–143, 2016

CSRR Inspired Conductor Backed CPW-Fed Monopole Antenna for Multiband Operation

Rajasekar Boopathi Rani[1, *] and Shashi K. Pandey[2]

Abstract—A conductor backed coplanar waveguide (CPW) fed multiband antenna inspired by CSRR MTM is presented. The shorting of ground in CPW feed and conductor backed arrangement extend the area of ground plane. The proposed antenna consists of rectangular monopole with Complementary Split Ring Resonator (CSRR) engraved in the extended ground plane. The prototype antenna is designed, fabricated and measured. CSRR characteristics are also analyzed. Simulated and measured results of the antenna are in good agreement with each other and are discussed. The proposed antenna can be used for WiMAX, WLAN and RADAR applications at 3.4 GHz, 5.16 GHz and 9.5 GHz, respectively.

1. INTRODUCTION

With the advent of modern gadgets along with wireless interconnectivity and wide range of applications, there has been an embryonic necessity for an antenna to work in multiband. The desire for more compact, lightweight, handy equipment makes the most optimum choice for an antenna as planar antenna. The conventional way of making an antenna with heavy, bigger pole or larger aperture is replaced by planar form in many applications. There are different forms of planar antennas reported in literature for single, dual/multi-band and wideband. Having an antenna that operates at two distinct bands not only reduces space and cost of two single band antenna but also reduces interference when single wideband antenna is used to cover both the bands.

There are different techniques devised to realize multiband antenna. The techniques such as having different lengths of pole [1–4], shorting pin [5, 6], shorting plate [7], slot [8, 9], fractal [10], fractal slot [11] have been used in realizing dual/multi-band or wideband antenna. This paper analyses the role of metamaterial (MTM) in achieving multiband antenna. MTM is a class of artificial material which provides properties that are not readily available in nature [12, 13]. MTM achieves properties from its structural composition rather than from the constituent material. MTM has been used in antenna in a variety of forms to achieve enhanced performance.

MTM was used to realize miniature antenna [14–16]. Keeping MTM between patch and ground [17] and CSRR loaded ground of microstrip fed antenna [18] results in gain enhancement. A monopole antenna using composite MTM [19], an array of thin wire [20], and inclusion of transmission line MTM on patch [21] exhibited broadband response. SRR was loaded in the ground plane of a monopole antenna for achieving broadband impedance matching [22].

An ultrawideband with notch band has been proposed by including CSRR on microstrip-fed patch of an antenna [23]. An antenna radiation pattern was improved by including dual-ring square-shaped SRR [24] and single/multi-ring rhombus-shaped SRR [25] in ground plane. Zeroth-Order Resonant (ZOR) MTM loaded circular sector antenna exhibited good radiation performance [26]. OCSRRs were included in radiating patch [27], and OCSRR included patch with modified ground plane [28]

Received 28 October 2016, Accepted 18 December 2016, Scheduled 5 January 2017

* Corresponding author: Rajasekar Boopathi Rani (rbrani@nitpy.ac.in).

[1] Department of Electronics and Communication Engineering, National Institute of Technology Puducherry, India. [2] National Institute of Technology Puducherry, India.

was proposed to achieve multiband antenna. ZOR and CSRR loaded antenna exhibited multiband operation [29]. There are many different structures presented in literature for realizing MTM. Among them, the rectangle-shaped two-slot CSRR follows a simple geometry. This paper presents the outcomes of inclusion of CSRR MTM in realizing multiband antenna. The proposed antenna and CSRR on ground follow a straightforward design approach. As the antenna is fed by CPW-feed, the CSRR is engraved on the extended ground plane on the other side of the substrate. This technique achieves an antenna which will result in multiband operation.

2. ANTENNA STRUCTURE AND DESIGN

The initial design of an antenna is aimed to get one resonance (Step-1). Then the ground plane area is extended by backing conductor on the bottom side of the substrate (Step-2). In the extended ground plane, a rectangular 2-slot CSRR is formed by etching some portion of the conductor (Step-3). The top and bottom sides of the proposed antenna are given in Figure 1. An FR4 material having dielectric constant 4.4 and loss tangent 0.02 is used as a substrate. FR4 material is chosen for substrate due to its easy availability and cost effectiveness. Thickness of the substrate is 1.6 mm.

The antenna discussed in this paper is a rectangular monopole antenna fed by a 50 Ω coplanar waveguide. The basic design equations are given in [30–32]. Computer program is written for finding initial dimensions of the proposed antenna. The dimensions are $W_S = 31$ mm, $L_S = 26.27$ mm, $W_P = 12.6$ mm, $L_P = 13.97$ mm, $W_g = 14.5$ mm, $L_g = 9.8$ mm, $W_f = 1.6$ mm, $L_f = 10.6$ mm and $g = 0.2$ mm. Initially, the rectangular monopole is designed to operate the antenna at 4.7 GHz. Then, the ground area is extended by placing another conductor on the other side of the substrate. Obviously, this arrangement will have effect on current distribution of antenna and slightly alter the resonance characteristics.

In order to further improve the return loss value, CSRR is introduced in the ground plane. CSRR is designed by having dimensions of $W_c = 8.2$ mm, $L_c = 5.09$ mm, outer and inner slot width of 0.8 mm and 0.7 mm, respectively. The distance between the outer and inner slots is 0.3 mm, and slit in the ring is 0.28 mm. The offset position of CSRR from the bottom left corner of the substrate is given as $W_o = 10.5$ mm and $L_o = 12.01$ mm from the left and bottom edges. The relation between medium properties and propagation constant is given in Equation (1) [33].

$$\beta = \omega\sqrt{\mu\epsilon} \tag{1}$$

From this, it is explicit that if the value of permeability μ or permittivity ϵ goes negative, then the propagation constant β becomes imaginary. CSRR provides effective negative value for permittivity [34–36]. This results in imaginary value for propagation constant which validates the loss due to transmission. Hence, in the regions of negative permittivity, it provides more transmission loss which is evident from Equation (1). CSRR also has resonance behaviour, it introduces stop band

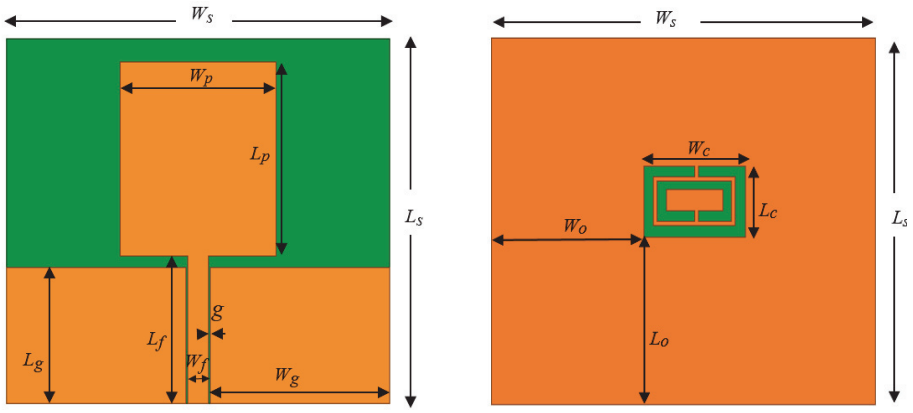

(a) (b)

Figure 1. Geometry of proposed antenna. (a) Top side; (b) Bottom side.

at some frequencies and pass band at other frequencies. The position of CSRR on the backside of the substrate is shown in Figure 1(b).

3. RESULTS AND DISCUSSIONS

The return loss (S_{11}) characteristics of all the three antenna configurations discussed in design process from steps 1 to 3 such as a monopole antenna with normal ground, with extended ground and with CSRR engraved in extended ground are shown in Figure 2(a). It has been observed that the extended area of ground plane not only modifies the return loss characteristics and induces resonance at 5.16 GHz, 6.99 GHz and 9.56 GHz but also necessitates improvement in impedance matching. The inclusion of CSRR in extended ground plane slightly alters the resonance frequencies, induces one more resonance at 3.4 GHz and further improves the return loss. The shift in resonant frequency attributes to the cumulative effect of CSRR and monopole resonances. Further, inclusion of CSRR, improves the impedance matching and impedance bandwidth. The simulation setup of CSRR is given in Figure 3(a) which depicts the waveguide arrangement to find the transmission loss (S_{21}) and return loss (S_{11}) characteristics of CSRR.

The design and excitation details of CSRR are as follows: CSRR is the complementary structure of SRR. Both SRR and CSRR can be compared using duality principle. The CSRR has a metallic portion which is complement (dual) to the metallic portion present in SRR. Both are resonating structures. The design of CSRR is similar to that of SRR with complementary operation. The design equations used in the design of SRR can be used for the design of CSRR. The CSRR exhibits negative permittivity in the same frequency region where SRR exhibits negative permeability. Similarly, the excitation of perfect-E and perfect-H are also in complementary directions as illustrated in Figure 3(a). The interested readers are directed to [34–36] for detailed information on CSRR.

Excitation direction and boundary conditions are mentioned in Figure 3(a). This shows that the perfect-E boundary is specified in Z-plane, perfect-H boundary is assigned in X-plane and excitation is given in Y-plane of the bounding box of CSRR. The return loss (S_{11}) and transmission loss (S_{21}) characteristics of CSRR are given in Figure 3(b). The transmission loss (S_{21}) of any component denotes the reduction in signal strength while passing through that component. The return loss (S_{11}) denotes the amount of power reflected from the component at its ports. Normally at the resonant frequency of antenna, the return loss should be less than -10 dB and there should not be any transmission loss. The S_{21} characteristics of CSRR illustrates stop band from 3.6 GHz to 6.34 GHz and 6.93 GHz to 9.4 GHz. It is evident from Figure 3(b) that CSRR accounts for resonance at 3.4 GHz and 9.5 GHz and extended ground accounts for resonance at 5.16 GHz with good return loss.

A photograph of the fabricated antenna with connector is shown in Figure 4. The proposed antenna is connected with *Sub-Miniature-A* (SMA) connector which has VSWR of 1.08 upto 15 GHz. This connector is chosen because it provides good matching to frequencies upto 15 GHz range. Here, the top

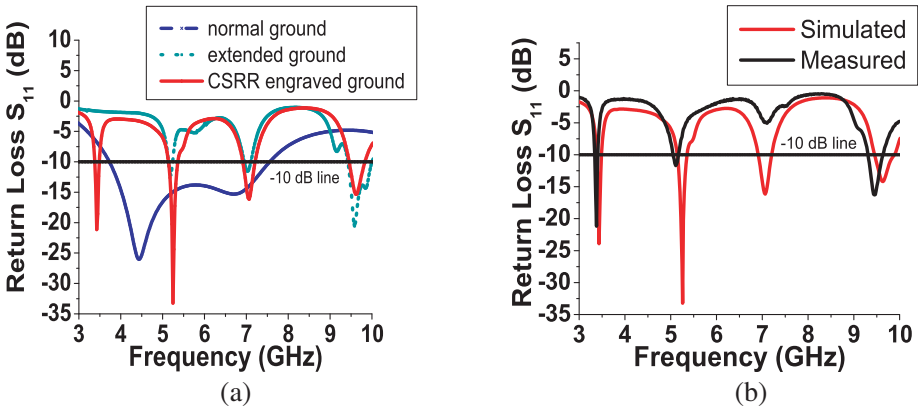

Figure 2. Return loss S_{11} plot. (a) S_{11} for different ground configuration; (b) Simulated and measured S_{11}.

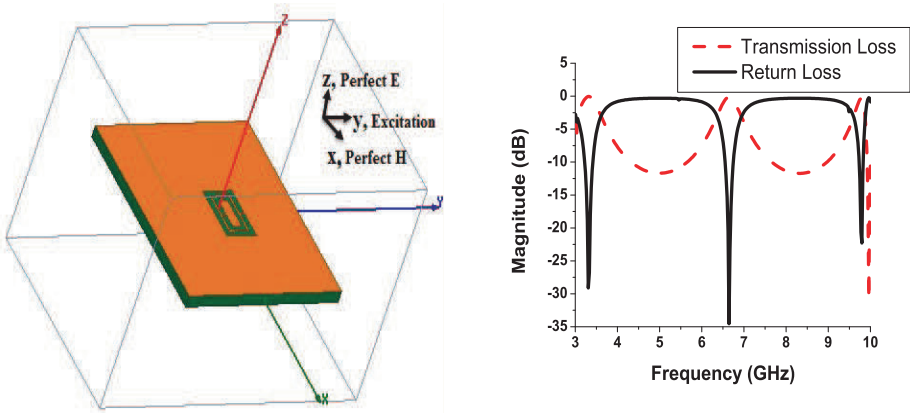

(a) (b)

Figure 3. CSRR simulation and its characteristics plot. (a) CSRR simulation, waveguide setup; (b) CSRR transmission and return loss characteristics.

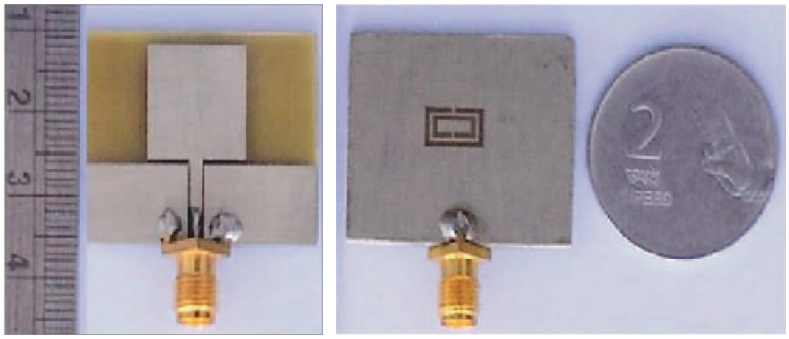

(a) (b)

Figure 4. Photograph of fabricated antenna. (a) Top view; (b) Bottom view.

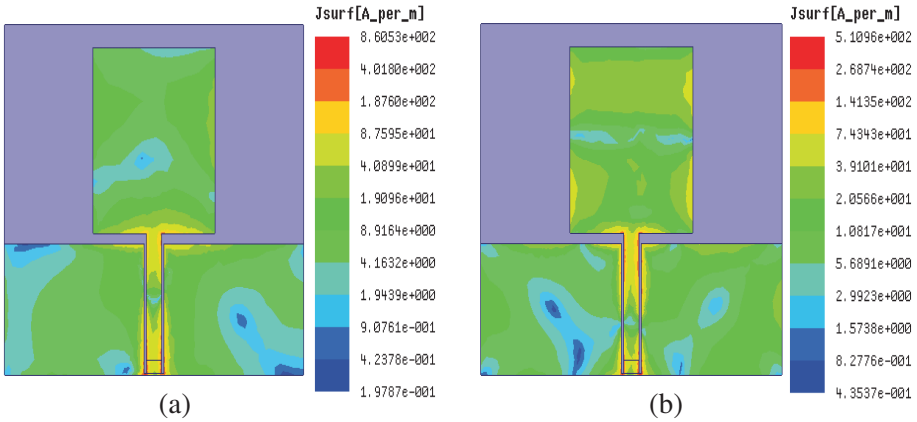

(a) (b)

Figure 5. Surface current distribution on antenna. (a) At 7.03 GHz; (b) At 9.5 GHz.

side of an antenna along with normal scale and the bottom side an antenna along with an Indian Rs.2 coin for comparative appraisal purpose. The return loss characteristics of designed antenna is found using simulation and is measured using vector network analyser which is displayed in Figure 2(b). The measured impedance bandwidth are 100 MHz (3.33–3.43 GHz), 240 MHz (5.03–5.27 GHz) and 350 MHz (9.30–9.65 GHz) with resonance frequencies at 3.37 GHz, 5.16 GHz and 9.45 GHz respectively. The potential band observed at 7.03 GHz in simulation is not present with required minimum return loss

value in measurement but a small dip is observed at this band. To analyze the reason for this behaviour of an antenna, the surface current distribution on antenna at 7.03 GHz and 9.5 GHz is plotted since both exhibit almost equal amount of return loss in simulation. These are respectively shown in Figure 5(a) and Figure 5(b). It can be read from Figure 5(b) that at 9.5 GHz the more current is observed at outer edges, center of patch and ground whereas in Figure 5(a), at 7.03 GHz the current distribution is more at crucial places which is limited by fabrication accuracy i.e., edges which are present at the junction near feed, ground and patch. Hence, the reason for non-observance of potential band at 7.03 GHz in measurement may attribute to limitation in fabrication precision at the junction. The far-field radiation patterns of the antenna are measured by keeping an antenna inside an anechoic chamber having 8-m distance between transmitting and receiving antennas. This is carried out at two different resonating frequencies namely 3.4 GHz and 5.1 GHz for 360° rotation of receiving antenna at two different angles of phi(90° and 0°) respectively for E-plane and H-plane measurements. These are shown in Figure 6 and Figure 7. As well as, the simulated far-field E-plane and H-plane patterns are shown in Figure 8. These depict that the far-field pattern is good and impersonates the behaviour of the intended dipole antenna pattern. The gain at various resonating frequencies is plotted in Figure 9 as red line. The minimum gain of the antenna is measured as 3.5 dBi in the frequencies of operation. The radiation efficiency denotes the percentage of power radiated when compared to input power to the antenna. This is plotted in Figure 9 as blue line.

The proposed antenna resonates at 3.4 GHz, 5.16 GHz and 9.5 GHz frequencies. The comparison to existing literature cannot be accurately made because the same set of frequency bands are not reported. Hence, the area requirement of patch is calculated using Equations (2) to (4) for each resonating

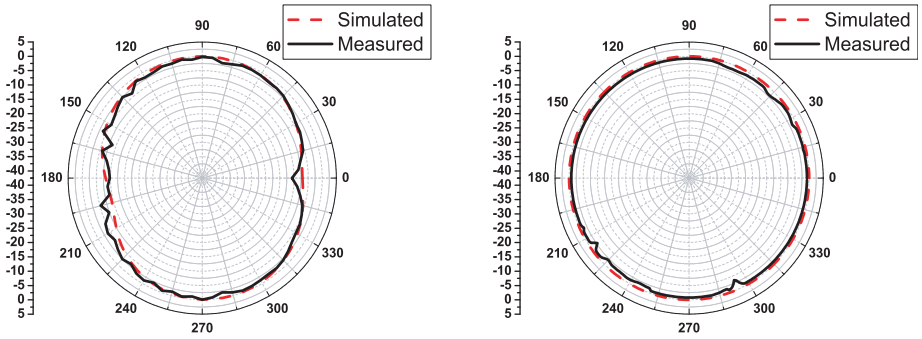

Figure 6. Far-field radiation patterns of the proposed antenna at 3.4 GHz. (a) E-plane pattern; (b) H-plane pattern.

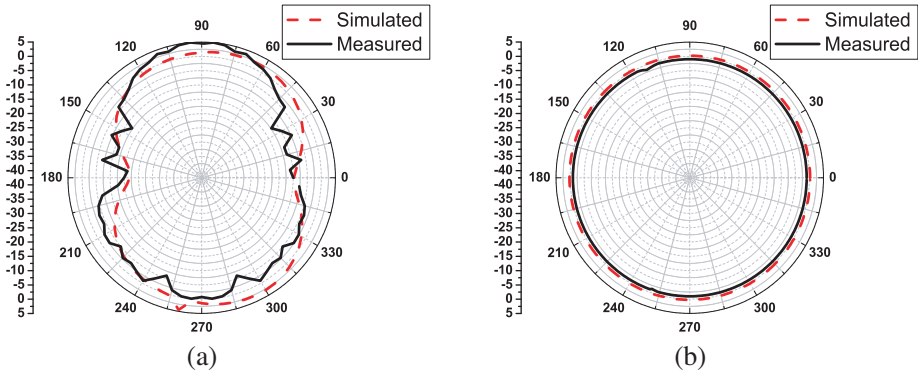

Figure 7. Far-field radiation patterns of the proposed antenna at 5.1 GHz. (a) E-plane pattern; (b) H-plane pattern.

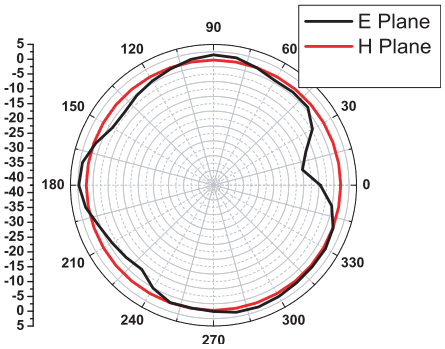

Figure 8. Simulated far-field radiation patterns of the proposed antenna at 9.5 GHz.

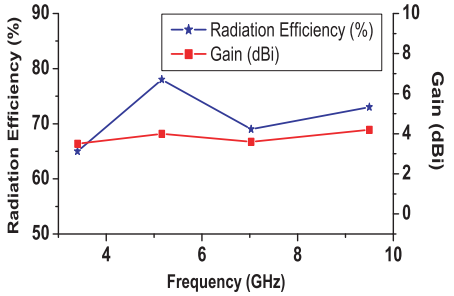

Figure 9. Gain and radiation efficiency of an antenna over frequency.

frequency and presented in Table 1.

$$W = \frac{c}{2f_r}\sqrt{\frac{2}{\epsilon_r + 1}} \tag{2}$$

$$\epsilon_{reff} = \frac{\epsilon_r + 1}{2} + \frac{\epsilon_r - 1}{2}\left[1 + 12\frac{h}{W}\right]^{-1/2} \tag{3}$$

$$L = \frac{\lambda}{2} - 0.824h\frac{(\epsilon_{reff} + 0.3)\left(\frac{W}{h} + 0.264\right)}{(\epsilon_{reff} - 0.258)\left(\frac{W}{h} + 0.8\right)} \tag{4}$$

where ϵ_r, ϵ_{reff}, c, f_r, λ and h respectively denote relative permittivity of substrate, effective relative permittivity, velocity of light in free space, resonating frequency, free space wavelength and height of the substrate. W and L respectively denote width and length of the patch.

Table 1. Patch area requirement.

Antenna f_r (GHz)	**Dimension (mm × mm)**	**Area (mm^2)**
3.4	26.8 × 20.6	552.08
5.16	17.8 × 13.3	236.74
9.5	9.6 × 6.8	65.28
Three single band antenna for above frequencies	∼ 54.2 × 40.7	854.1
The proposed antenna	13.97 × 12.6	176.02

From this, it can be inferred that the total patch area requirement for three single band antenna is 854.1 mm^2 whereas the proposed antenna patch occupies only 176.02 mm^2. Hence, compactness is achieved by using the technique of inclusion of CSRR at the backside of CPW fed antenna.

4. CONCLUSIONS

A multiband antenna using CSRR MTM has been presented. This is achieved by including CSRR MTM in the extended area of ground plane of CPW-feed. The transmission and return loss characteristics of CSRR are also plotted to validate the multiband operation of designed antenna. The antenna prototype has been fabricated and measured. The measured impedance bandwidth testifies that the designed antenna covers WiMAX, WLAN and RADAR applications at 3.4 GHz, 5.16 GHz and 9.5 GHz respectively. Good far-field patterns have been observed for the entire bands of operation.

ACKNOWLEDGMENT

The authors gratefully acknowledge Indian Space Research Organization (ISRO) Satellite Centre, Bangalore, India for their kind support in carrying out measurements of antenna characteristics.

REFERENCES

1. Kuo, Y. L. and K. L. Wong, "Printed double-T monopole antenna for 2.4/5.2 GHz dual-band WLAN operations," *IEEE Transactions on Antennas and Propagation*, Vol. 51, No. 9, 2187–2192, 2003, doi: 10.1109/TAP.2003.816391.
2. Mishra, S. K., R. K. Gupta, A. Vaidya, and J. Mukherjee, "A compact dual-band fork-shaped monopole antenna for bluetooth and UWB applications," *IEEE Antennas and Wireless Propagation Letters*, Vol. 10, 627–630, 2011, doi: 10.1109/LAWP.2011.2159572.
3. Sujith, R., V. Deepu, S. Mridula, B. Paul, D. Laila, and P. Mohanan, "Compact CPW-fed uniplanar antenna for multiband wireless applications," *AEU-International Journal of Electronics and Communications*, Vol. 65, No. 6, 553–559, 2011, doi: 10.1016/j.aeue.2010.09.006.
4. Kunwar, A. and A. K. Gautam, "Fork-shaped planar antenna for Bluetooth, WLAN, and WiMAX applications," *International Journal of Microwave and Wireless Technologies*, Vol. 8, 1–6, 2016, doi:10.1017/S1759078716000647.
5. Ahmad, M. S. and C. Y. Kim, "Dual-element PIFA design with dual shorting pins for multiband communication devices," *International Journal of Antennas and Propagation*, 1–8, 2015, doi: 10.1155/2015/742352.
6. Singh, A. K. and M. K. Meshram, "Shorting pin loaded dual-band compact rectangular microstrip antenna," *International Journal of Electronics*, Vol. 94, No. 3, 237–250, 2007, doi: 10.1080/00207210601108166.
7. Wong, K. L., L. C. Chou, and C. M. Su, "Dual-band flat-plate antenna with a shorted parasitic element for laptop applications," *IEEE Transactions on Antennas and Propagation*, Vol. 53, No. 1, 539–544, 2005, doi: 10.1109/TAP.2004.838754.
8. Ansal, K. A. and T. Shanmuganantham, "Compact ACS-fed antenna with DGS and DMS for WiMAX/WLAN applications," *International Journal of Microwave and Wireless Technologies*, Vol. 7, 1–6, 2015, doi: 10.1017/S1759078715000537.
9. Boopathi Rani, R. and S. K. Pandey, "A parasitic hexagonal patch antenna surrounded by same shaped slot for WLAN, UWB applications with notch at VANET frequency band," *Microwave and Optical Technology Letters*, Vol. 58, No. 12, 2996–3000, 2016, doi: 10.1002/mop.30204.
10. Singh, A. and S. Singh, "Design and optimization of a modified Sierpinski fractal antenna for broadband applications," *Applied Soft Computing*, Vol. 38, 843–850, 2016, doi: 10.1016/j.asoc.2015.10.013.
11. Ghatak, R., S. K. Ghoshal, D. Mondal, and A. K. Bhattacharjee, "A dual wideband Sierpinski carpet fractal-shaped planar monopole antenna with CPW feed," *International Journal of Microwave and Wireless Technologies*, Vol. 3, 77–79, 2011, doi: 10.1017/S1759078711000055.
12. Veselago, V. G., "The electrodynamics of substances with simultaneously negative values of ϵ and μ," *Soviet Physics Uspekhi*, Vol. 10, No. 4, 509–514, 1968, doi: 10.1070/PU1968v010n04ABEH003699.
13. Pendry, J. B., A. J. Holden, D. J. Robbins and W. J. Stewart, "Magnetism from conductors and enhanced nonlinear phenomena," *IEEE Transactions on Microwave Theory and Techniques*, Vol. 47, No. 11, 2075–2084, 1999, doi: 10.1109/22.798002.
14. Kim, T. G. and B. Lee, "Metamaterial-based compact zeroth-order resonant antenna," *Electronics Letters*, Vol. 45, No. 1, 12–13, 2009, doi: 10.1049/el:20092715.
15. Ouedraogo, R. O., E. J. Rothwell, A. R. Diaz, K. Fuchi, and A. Temme, "Miniaturization of patch antennas using a metamaterial-inspired techniques," *IEEE Transactions on Antennas and Propagation*, Vol. 60, No. 5, 2175–2182, 2012, doi: 10.1109/TAP.2012.2189699.

16. Sharawi, M. S., M. U. Khan, A. B. Numan, and D. N. Aloi, "A CSRR loaded MIMO antenna system for ISM band operation," *IEEE Transactions on Antennas and Propagation*, Vol. 61, No. 8, 4265–4274, 2013, doi: 10.1109/TAP.2013.2263214.
17. Majid, H. A., M. K. Abd Rahim, and T. Masri, "Microstrip antenna's gain enhancement using left-handed metamaterial structure," *Progress In Electromagnetics Research M*, Vol. 8, 235–247, 2009.
18. Pandeeswari, R. and S. Raghavan, "Microstrip antenna with complementary split ring resonator loaded ground plane for gain enhancement," *Microwave and Optical Technology Letters*, Vol. 57, No. 2, 292–296, 2015, doi:10.1002/mop.28835.
19. Si, L.-M. and X. Lv, "CPW-fed multi-band omni-directional planar microstrip antenna using composite metamaterial resonators for wireless communications," *Progress In Electromagnetics Research*, Vol. 83, 133–146, 2008.
20. Anila, P. V., K. K. Indhu, C. M. Nijas, R. Sujith, S. Mridula, and P. Mohanan, "A planar compact metamaterial-inspired broadband antenna," *Microwave and Optical Technology Letters*, Vol. 56, No. 3, 610–613, 2014, doi:10.1002/mop.28175.
21. Zhu, J. and G. V. Eleftheriades, "A compact transmission-line metamaterial antenna with extended bandwidth," *IEEE Antennas and Wireless Propagation Letters*, Vol. 8, 295–298, 2009, doi: 10.1109/LAWP.2008.2010722.
22. Pandeeswari, R. and S. Raghavan, "Broadband monopole antenn with split ring resonator loaded substrate for good impedance matching," *Microwave and Optical Technology Letters*, Vol. 56, No. 10, 2388–2392, 2014, doi: 10.1002/mop.28602.
23. Mishra, G. and S. Sahu, "Compact circular patch UWB antenna with WLAN band notch characteristics," *Microwave and Optical Technology Letters*, Vol. 58, No. 5, 1068–1073, 2016, doi:10.1002/mop.29727.
24. Patel, S. K. and Y. Kosta, "Investigation on radiation improvement of corner truncated square microstrip patch antenna with double negative material," *Journal of Electromagnetic Waves and Applications*, Vol. 27, No. 7, 819–833, 2013, doi: 10.1080/09205071.2013.789407.
25. Naoui, S., L. Latrach, and A. Gharsallah, "Metamaterials microstrip patch antenna for wireless communication RFID Technology," *Microwave and Optical Technology Letters*, Vol. 57, No. 5, 1060–1066, 2015, doi: 10.1002/mop.29016.
26. Yan, S. and G. A. E. Vandenbosch, "Meta-loaded circular sector patch antenna," *Progress In Electromagnetics Research*, Vol. 156, 37–46, 2016.
27. Herraiz-Martinez, F. J., G. Zamora, F. Paredes, F. Martin, and J. Bonache, "Multiband printed monopole antennas loaded with OCSRRs for PANs and WLANs," *IEEE Antennas and Wireless Propagation Letters*, Vol. 10, 1528–1531, 2011, doi: 10.1109/LAWP.2011.2181309.
28. Pandeeswari, R. and S. Raghavan, "A CPW-fed triple band OCSRR embedded monopole antenna with modified ground for WLAN and WIMAX applications," *Microwave and Optical Technology Letters*, Vol. 57, No. 10, 2413–2418, 2015, doi: 10.1002/mop.29352.
29. Mehdipour, A., T. A. Denidni, and A. R. Sebak, "Multi-band miniaturized antenna loaded by ZOR and CSRR metamaterial structures with monopolar radiation pattern," *IEEE Transactions on Antennas and Propagation*, Vol. 62, No. 2, 555–562, 2014, doi: 10.1109/TAP.2013.2290791.
30. Garg, R., P. Bhartia, I. Bahl, and A. Ittipiboon, *Microstrip Antenna Design Handbook*, Artech House, 2001, ISBN-13: 978-0890065136.
31. Wong, K. L., *Compact and Broadband Microstrip Antennas*, Wiley, 2002, ISBN-13: 978-0471417173.
32. Balanis, C. A., *Antenna Theory, Analysis and Design*, 3rd Edition, Wiley, New York, USA, 2005, ISBN-13: 978-0471667827.
33. Hwang, J. N. and F. C. Chen, "Reduction of the peak SAR in the human head with metamaterials," *IEEE Transactions on Antennas and Propagation*, Vol. 54, No. 12, 3763–3770, 2006, doi:10.1109/TAP.2006.886501.

34. Baena, J. D., J. Bonache, F. Martn, R. M. Sillero, F. Falcone, T. Lopetegi, M. A. G. Laso, J. Garcia-Garca, I. Gil, M F. Portillo, and M. Sorolla, "Equivalent-circuit models for split-ring resonators and complementary split-ring resonators coupled to planar transmission lines," *IEEE Transactions on Microwave Theory and Techniques*, Vol. 53, No. 4, 1451–1461, 2005, doi:10.1109/TMTT.2005.845211.
35. Falcone, F., T. Lopetegi, J. D. Baena, R. Marqus, F. Martn, and M. Sorolla, "Effective negative-ϵ stopband microstrip lines based on complementary split ring resonators," *IEEE Microwave and Wireless Components Letters*, Vol. 14, No. 6, 280–282, 2004, doi:10.1109/LMWC.2004.828029.
36. Bonache, J., M. Gil, I. Gil, J. Garcia-Garcia, and F. Martin, "On the electrical characteristics of complementary metamaterial resonators," *IEEE Microwave and Wireless Components Letters*, Vol. 16, No. 10, 543–545. 2006, doi:10.1109/LMWC.2006.882400.